Formation of Stellar Clusters and the Importance of Thermodynamics for Fragmentation

Ralf S. Klessen[1], Paul C. Clark[1] and Simon C. O. Glover[2]

[1]Zentrum für Astronomie der Universität Heidelberg, Institut für Theoretische Astrophysik, Albert-Ueberle-Str. 2, 69120 Heidelberg, Germany

[2]Astrophysikalisches Institut Potsdam, An der Sternwarte 16, 14482 Potsdam, Germany

Abstract. We discuss results from numerical simulations of star cluster formation in the turbulent interstellar medium (ISM). The thermodynamic behavior of the star-forming gas plays a crucial role in fragmentation and determines the stellar mass function as well as the dynamic properties of the nascent stellar cluster. This holds for star formation in molecular clouds in the solar neighborhood as well as for the formation of the very first stars in the early universe. The thermodynamic state of the ISM is a result of the balance between heating and cooling processes, which in turn are determined by atomic and molecular physics and by chemical abundances. Features in the effective equation of state of the gas, such as a transition from a cooling to a heating regime, define a characteristic mass scale for fragmentation and so set the peak of the initial mass function of stars (IMF). As it is based on fundamental physical quantities and constants, this is an attractive approach to explain the apparent universality of the IMF in the solar neighborhood as well as the transition from purely primordial high-mass star formation to the more normal low-mass mode observed today.

Keywords. stars: formation – stars: mass function – early universe – hydrodynamics – equation of state – methods: numerical

1. Introduction

Identifying the physical processes that determine the masses of stars and their statistical distribution, the initial mass function (IMF), is a fundamental problem in star-formation research. It is central to much of modern astrophysics, with implications ranging from cosmic re-ionisation and the formation of the first galaxies, over the evolution and structure of our own Milky Way, down to the build-up of planets and planetary systems.

Near the Sun the number density of stars as a function of mass has a peak at a characteristic stellar mass of a few tenths of a solar mass, below which it declines steeply, and for masses above one solar mass it follows a power-law with an exponent $dN/d\log m \propto m^{-1.3}$. Within a radius of several kpc this distribution shows surprisingly little variation (Salpeter 1955; Scalo 1998; Kroupa 2001; Kroupa 2002; Chabrier 2003). This has prompted the suggestion that the distribution of stellar masses at birth is a truly universal function, which often is referred to as the Salpeter IMF, although note that the original Salpeter (1955) estimate was a pure power-law fit without characteristic mass scale.

The initial conditions in star forming regions can vary considerably, even in the solar vicinity. If the IMF were to depend on the initial conditions, there would be no reason for it to be universal. Therefore a derivation of the characteristic stellar mass that is based on fundamental atomic and molecular physics would be highly desirable. In

this proceedings contribution we argue that indeed the thermodynamic properties of the star-forming cloud material determine the characteristic mass scale for fragmentation and subsequent stellar birth. The thermodynamic state of interstellar gas is a result of the balance between heating and cooling processes, which in turn are determined by fundamental atomic and molecular physics and by chemical abundances. The derivation of a characteristic stellar mass can thus be based on quantities and constants that depend solely on the chemical abundances in a molecular cloud. It also explains why deviations from the "standard" mode of star formation are likely to occur under extreme environmental conditions such as those occurring in the early universe or in circum-nuclear starburst regions.

2. Gravoturbulent Star Cluster Formation

Stars and star clusters form through the interplay between self-gravity on the one hand and turbulence, magnetic fields, and thermal pressure on the other (for recent reviews see Larson 2003; Mac Low & Klessen 2004; Ballesteros-Paredes *et al.* 2006). Supersonic turbulence, even if it is strong enough to counterbalance gravity on global scales, will usually *provoke* local collapse. Turbulence establishes a complex network of interacting shocks, where converging shock fronts generate clumps of high density. These density enhancements can be large enough for the fluctuations to become gravitationally unstable and collapse, which can occur when the local Jeans length becomes smaller than the size of the fluctuation. However, the fluctuations in turbulent velocity fields are highly transient. The random flow that creates local density enhancements can disperse them again. For local collapse to actually result in the formation of stars, Jeans-unstable shock-generated density fluctuations must collapse to sufficiently high densities on time scales shorter than the typical time interval between two successive shock passages. Only then are they able to 'decouple' from the ambient flow and survive subsequent shock interactions. The shorter the time between shock passages, the less likely these fluctuations are to survive. Hence, the timescale and efficiency of protostellar core formation depend strongly on the wavelength and strength of the driving source as well as on the dynamic response of the gas, as defined by the equation of state, i.e. the balance between heating and cooling processes.

The velocity field of long-wavelength turbulence is found to be dominated by large-scale shocks which are very efficient in sweeping up molecular cloud material, thus creating massive coherent structures. When a coherent region reaches the critical density for gravitational collapse, its mass typically exceeds the local Jeans limit by far. Inside the shock compressed region, the velocity dispersion is much smaller than in the ambient turbulent flow and the situation is similar to localized turbulent decay. These are the conditions for the formation of star clusters. The efficiency of turbulent fragmentation is reduced if the driving wavelength decreases. When energy is inserted mainly on small spatial scales, the network of interacting shocks is very tightly knit, and protostellar cores form independently of each other at random locations throughout the cloud and at random times. Individual shock-generated clumps have lower mass and the time interval between two shock passages through the same point in space is small. Collapsing cores are easily destroyed again and the resulting mass spectrum shows deviations from the observed IMF. All this points toward interstellar gas clouds being driven on large scales.

Altogether, stellar birth is intimately linked to the dynamic behavior of the parental gas cloud, which governs when and where star formation sets in. The chemical and thermodynamic properties of interstellar clouds play a key role in this process. In particular, the value of the polytropic exponent γ, when adopting an EOS of the form $P \propto \rho^\gamma$,

strongly influences the compressibility of density condensations as well as the temperature of the gas. The EOS thus determines the amount of clump fragmentation, and so directly relates to the IMF (Vázquez-Semadeni *et al.* 1996) with values of γ larger than unity leading to little fragmentation and high mass cores (Li, Klessen, & Mac Low 2003; Jappsen *et al.* 2005). The stiffness of the EOS in turn depends strongly on the ambient metallicity, density and infrared background radiation field produced by warm dust grains. The EOS thus varies considerably in different galactic environments (see Spaans & Silk 2000, 2005 for a detailed account).

3. Formation of Stellar Clusters in the Solar Neighborhood

Early studies of the balance between heating and cooling processes in collapsing clouds predicted temperatures of the order of $10\,\mathrm{K}$ to $20\,\mathrm{K}$, tending to be lower at the higher densities (e.g., Hayashi & Nakano 1965; Hayashi 1966; Larson 1969, 1973b). In their dynamical collapse calculations, these and other authors approximated this somewhat varying temperature by a simple constant value, usually taken to be $10\,\mathrm{K}$. Nearly all subsequent studies of cloud collapse and fragmentation have used a similar isothermal approximation. However, this approximation is actually only a somewhat crude one, valid only to a factor of 2, since the temperature is predicted to vary by this much above and below the usually assumed constant value of $10\,\mathrm{K}$. Given the strong sensitivity of the results of fragmentation simulations like those of Li *et al.* (2003) to the assumed equation of state of the gas, temperature variations of this magnitude may be important for quantitative predictions of stellar masses and the IMF.

As can be seen in Fig. 2 of Larson (1985), observational and theoretical studies of the thermal properties of collapsing clouds both indicate that at densities below about $10^{-18}\,\mathrm{g\,cm^{-3}}$, roughly corresponding to a number density of $n = 2.5 \times 10^5\,\mathrm{cm^{-3}}$, the temperature generally decreases with increasing density. In this low-density regime, clouds are externally heated by cosmic rays or photoelectric heating, and they are cooled mainly by the collisional excitation of low-lying levels of C^+ ions and O atoms; the strong dependence of the cooling rate on density then yields an equilibrium temperature that decreases with increasing density. The work of Koyama & Inutsuka (2000), which assumes that photoelectric heating dominates, rather than cosmic ray heating as had been assumed in earlier work, predicts a very similar trend of decreasing temperature with increasing density at low densities. The three-dimensional magnetohydrodynamic simulations of Glover & Mac Low (2007) also produce a similar result, although in this case the point-to-point scatter is larger. The resulting temperature-density relation can be approximated by a power law with an exponent of about -0.275, which corresponds to a polytropic equation of state with $\gamma = 0.725$. The observational results of Myers (1978) shown in Fig. 2 of Larson (1985) suggest temperatures rising again toward the high end of this low-density regime, but those measurements refer mainly to relatively massive and warm cloud cores and not to the small, dense, cold cores in which low-mass stars form. As reviewed by Evans (1999), the temperatures of these cores are typically only about $8.5\,\mathrm{K}$ at a density of $10^{-19}\,\mathrm{g\,cm^{-3}}$, consistent with a continuation of the decreasing trend noted above and with the continuing validity of a polytropic approximation with $\gamma \approx 0.725$ up to a density of at least $10^{-19}\,\mathrm{g\,cm^{-3}}$.

At higher densities, atomic line cooling becomes less effective as the cooling rates start to reach their local thermodynamic equilibrium (LTE) limits and as the line opacities grow larger. Consequently, at densities above $10^{-18}\,\mathrm{g\,cm^{-3}}$ the gas becomes thermally coupled to the dust grains, which then control the temperature by their far-infrared thermal emission. In this high-density regime, dominated thermally by the dust, there

are few direct temperature measurements because the molecules normally observed freeze out onto the dust grains, but most of the available theoretical predictions are in good agreement concerning the expected thermal behavior of the gas (Larson 1973b; Low & Lynden-Bell 1976; Masunaga & Inutsuka 2000; Larson 2005). The balance between compressional heating and thermal cooling by dust results in a temperature that increases slowly with increasing density, and the resulting temperature-density relation can be approximated by a power law with an exponent of about 0.075, which corresponds to $\gamma = 1.075$. Between the low-density and the high-density regimes, the temperature is predicted to reach a minimum of $5\,\mathrm{K}$ at a density of about $2 \times 10^{-18}\,\mathrm{g\,cm^{-3}}$, at which point the Jeans mass is about $0.3\,M_\odot$. The actual minimum temperature reached is somewhat uncertain because observations have not yet confirmed the predicted very low values, but such cold gas would be very difficult to observe; various efforts to model the observations have suggested central temperatures between $6\,\mathrm{K}$ and $10\,\mathrm{K}$ for the densest observed prestellar cores, whose peak densities may approach $10^{-17}\,\mathrm{g\,cm^{-3}}$ (e.g. Zucconi *et al.* 2001; Evans *et al.* 2001; Tafalla *et al.* 2004). A power-law approximation to the equation of state with $\gamma \approx 1.075$ is expected to remain valid up to a density of about $10^{-13}\,\mathrm{g\,cm^{-3}}$, above which increasing opacity to the thermal emission from the dust causes the temperature to begin rising much more rapidly, resulting in an "opacity limit" on fragmentation that is somewhat below $0.01\,M_\odot$ (Low & Lynden-Bell 1976; Masunaga & Inutsuka 2000).

Adopting the piecewise polytropic equation of state outlined above, Jappsen *et al.* (2005) showed that the changing γ from a value below unity to one somewhat above unity at a critical density n_c influences the number of protostellar objects. If the critical density increases then more protostellar objects form but the mean mass decreases. Consequently, the peak of the resulting mass spectrum moves to lower masses with increasing critical density. This spectrum not only shows a pronounced peak but also a power-law tail towards higher masses. Its behavior is thus similar to the observed IMF.

A simple scaling argument based on the Jeans mass M_J at the critical density n_c leads to $M_\mathrm{ch} \propto n_\mathrm{c}^{-0.95}$. If there is a close relation between the average Jeans mass and the characteristic mass of a fragment, a similar relation should hold for the expected peak of the mass spectrum. The simulations by Jappsen *et al.* (2005) qualitatively support this hypothesis, but find a weaker density dependency $M_\mathrm{ch} \propto n_\mathrm{c}^{-0.5\pm0.1}$.

4. Formation of Stellar Clusters in the Early Universe

The formation of the first and second generations of stars in the early universe has far-reaching consequences for cosmic reionization and galaxy formation (Loeb & Barkana 2001; Bromm & Loeb 2004; Glover 2005). The physical processes that govern stellar birth in a metal-free or metal-poor environment, however, are still very poorly understood. Numerical simulations of the thermal and dynamical evolution of gas in primordial protogalactic halos indicate that the metal-free first stars, the so called Population III, are expected to be very massive, with masses anywhere in the range 20–$2000\,M_\odot$ (Abel, Bryan, & Norman 2002; Bromm, Coppi, & Larson 2002; Yoshida *et al.* 2006; O'Shea & Norman 2007), much larger than the characteristic mass scale found in the local IMF.

This means that at some stage of cosmic evolution there must have been a transition from primordial, high-mass star formation to the "normal" mode of star formation that dominates today. The discovery of extremely metal-poor subgiant stars in the Galactic halo with masses below one solar mass (Christlieb *et al.* 2002; Beers & Christlieb 2005) indicates that this transition occurs at abundances considerably smaller than the solar value. At the extreme end, these stars have iron abundances less than $10^{-5}\,\mathrm{Z_\odot}$, and
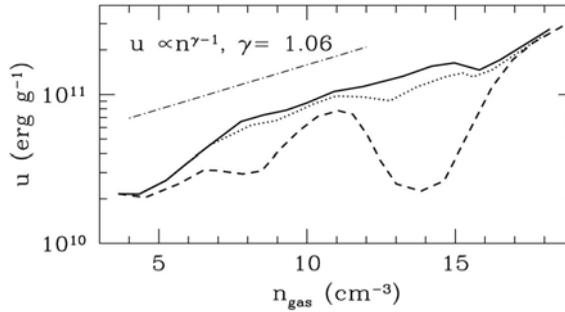
Figure 1. Three equations of state (EOSs) from Omukai *et al.* (2005) for different metallicities used by Clark, Glover, & Klessen (2007). The primordial case (solid line), $Z = 10^{-6} Z_\odot$ (dotted line), and $Z = 10^{-5} Z_\odot$ (dashed line), are shown alongside an example of a polytropic EOS with an effective $\gamma = 1.06$.

carbon or oxygen abundances that are still $\lesssim 10^{-3}$ the solar value. These stars are thus strongly iron deficient, which could be due to unusual abundance patterns produced by enrichment from pair-instability supernovae (Heger & Woosley 2002) from Population III stars or due to mass transfer from a close binary companion (Ryan *et al.* 2005; Komiya *et al.* 2007). There are hints for an increasing binary fraction with decreasing metallicity for these stars (Lucatello *et al.* 2005).

If metal enrichment is the key to the formation of low-mass stars, then logically there must be some critical metallicity Z_{crit} at which the formation of low mass stars first becomes possible. However, the value of Z_{crit} is a matter of ongoing debate. Some models suggest that low mass star formation becomes possible only once atomic fine-structure line cooling from carbon and oxygen becomes effective (Bromm *et al.* 2001; Bromm & Loeb 2003; Santoro & Shull 2006; Frebel, Johnson, & Bromm 2007), setting a value for Z_{crit} at around $10^{-3.5} Z_\odot$. Another possibility is that low mass star formation is a result of dust-induced fragmentation occurring at high densities, and thus at a very late stage in the protostellar collapse (Schneider *et al.* 2002; Omukai *et al.* 2005; Schneider *et al.* 2006; Tsuribe & Omukai 2006). In this model, $10^{-6} \lesssim Z_{crit} \lesssim 10^{-4} Z_\odot$, where much of the uncertainty in the predicted value results from uncertainties in the dust composition and the degree of gas-phase depletion (Schneider *et al.* 2002, 2006).

Clark, Glover, & Klessen (2007) modeled star formation in the central regions of low-mass halos at high redshift adopting an EOS similar to Omukai *et al.* (2005). They focused on a high-density regime with $10^5 \, \text{cm}^{-3} \leqslant n \leqslant 10^{17} \, \text{cm}^{-3}$. They find that enrichment of the gas to a metallicity of only $Z = 10^{-5} Z_\odot$ dramatically enhances fragmentation. A typical time evolution is illustrated in Fig. 2. It shows several stages in the collapse process, spanning a time interval from shortly before the formation of the first protostar (as identified by the formation of a sink particle in the simulation) to 420 years afterwards. During the initial contraction, the cloud builds up a central core with a density of about $n = 10^{10} \, \text{cm}^{-3}$. This core is supported by a combination of thermal pressure and rotation. Eventually, the core reaches high enough densities to go into free-fall collapse, and forms a single protostar. As more high angular momentum material falls to the center, the core evolves into a disk-like structure with density inhomogeneities caused by low levels of turbulence. As it grows in mass, its density increases. When dust-induced cooling sets in, it fragments heavily into a tightly packed protostellar cluster within only a few hundred years. One can see this behavior in particle density-position plots in Fig. 3. The simulation is stopped 420 years after the formation of the first stellar object (sink
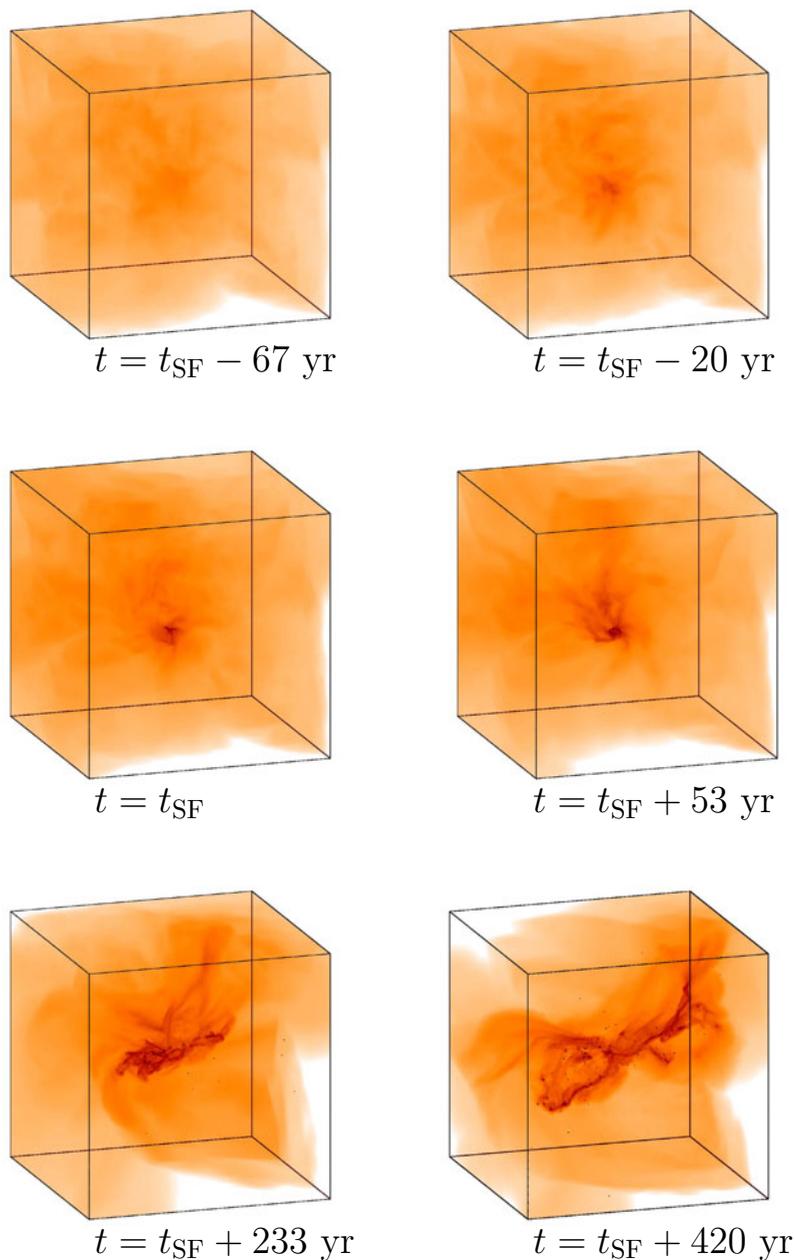
Figure 2. Time evolution of the density distribution in the innermost 400 AU of the proto-galactic halo shortly before and shortly after the formation of the first protostar at $t_{\rm SF}$. Only gas at densities above 10^{10} cm^{-3} are plotted. The dynamical timescale at a density $n = 10^{13}$ cm^{-3} is of the order of only 10 years. Dark dots indicate the location of protostars as identified by sink particles forming at $n \geqslant 10^{17}$ cm^{-3}. Note that without usage of sink particles to identify collapsed protostellar cores one would not have been able to follow the build-up of the proto-stellar cluster beyond the formation of the first object. There are 177 protostars when we stop the calculation at $t = t_{\rm SF} + 420$ yr. They occupy a region roughly a hundredth of the size of the initial cloud. With $18.7\,{\rm M}_\odot$ accreted at this stage, the stellar density is $2.25 \times 10^9\,{\rm M}_\odot\,{\rm pc}^{-3}$. Data are from Clark, Glover, & Klessen (2007).
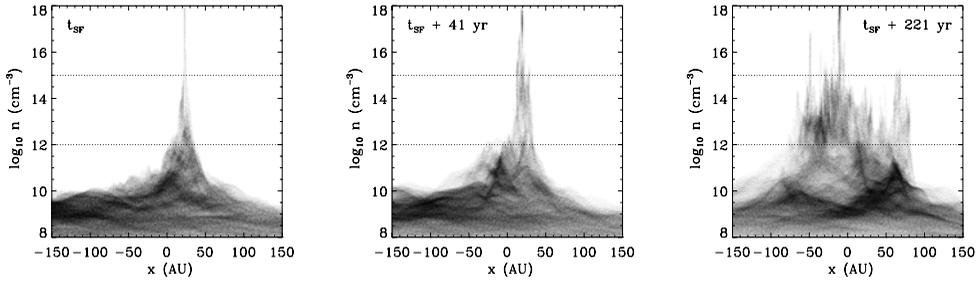
Figure 3. To illustrate the onset of the fragmentation process in the $Z = 10^{-5}$ $Z_\odot$ simulation, the graphs show the densities of the particles, plotted as a function of their x-position. Note that for each plot, the particle data has been centered on the region of interest. Results are plotted for three different output times, ranging from the time that the first star forms ($t_{\rm sf}$) to 221 years afterwards. The densities lying between the two horizontal dashed lines denote the range over which dust cooling lowers the gas temperature. The figure is from Clark, Glover, & Klessen (2007).

particle). At this point, the core has formed 177 stars. The evolution in the low-resolution simulation is very similar. The time between the formation of the first and second protostars is roughly 23 years, which is two orders of magnitude higher than the free-fall time at the density where the sinks are formed. Note that without the inclusion of sink particles, one would only have been able to capture the formation of the first collapsing object which forms the first protostar: the formation of the accompanying cluster would have been missed entirely.

The fragmentation of low-metallicity gas in this model is the result of two key features in its thermal evolution. First, the rise in the EOS curve between densities $10^9 \rm cm^{-3}$ and $10^{11} \rm cm^{-3}$ causes material to loiter at this point in the gravitational contraction. A similar behavior at densities around $n = 10^3 \rm\, cm^{-3}$ is discussed by Bromm *et al.* (2001), who call it a loitering phase. The rotationally stabilized disk-like structure, as seen in the plateau at $n \approx 10^{10} \rm cm^{-3}$ in Fig. 3, is able to accumulate a significant amount of mass in this phase and only slowly increases in density. Second, once the density exceeds $n \approx 10^{12} \rm cm^{-3}$, the sudden drop in the EOS curve lowers the critical mass for gravitational collapse by two orders of magnitude. The Jeans mass in the gas at this stage is only $M_{\rm J} = 0.01 \rm\, M_\odot$. The disk-like structure suddenly becomes highly unstable against gravitational collapse and fragments vigorously on timescales of several hundred years. A very dense cluster of embedded low-mass protostars builds up, and the protostars grow in mass by accretion from the available gas reservoir. The number of protostars formed by the end of the simulation is nearly two orders of magnitude larger than the initial number of Jeans masses in the cloud set-up.

Because the evolutionary timescale of the system is extremely short – the free-fall time at a density of $n = 10^{13} \rm\, cm^{-3}$ is of the order of 10 years – none of the protostars that have formed by the time that the simulation is stopped have yet commenced hydrogen burning. This justifies neglecting the effects of protostellar feedback in this study. Heating of the dust due to the significant accretion luminosities of the newly-formed protostars will occur (Krumholz 2006), but is unlikely to be important, as the temperature of the dust at the onset of dust-induced cooling is much higher than in a typical Galactic protostellar core ($T_{\rm dust} \sim 100 \rm\, K$ or more, compared to $\sim 10 \rm\, K$ in the Galactic case). The rapid collapse and fragmentation of the gas also leaves no time for dynamo amplification of magnetic fields (Tan & Blackman 2004), which in any case are expected to be weak and dynamically unimportant in primordial and very low metallicity gas (Widrow 2002).
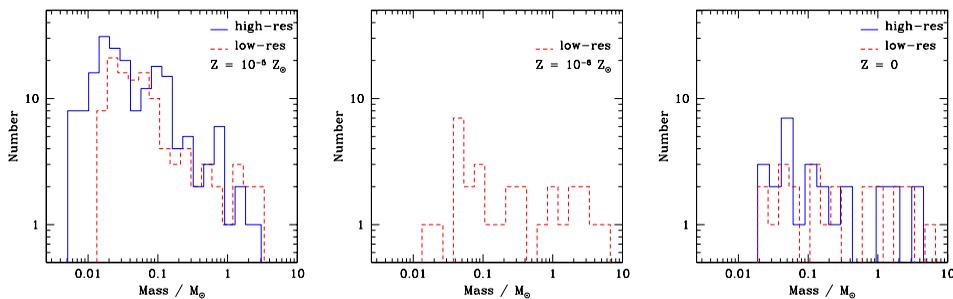
Figure 4. Mass functions resulting from simulations with metallicities $Z = 10^{-5}\,Z_\odot$ (left-hand panel), $Z = 10^{-6}\,Z_\odot$ (center panel), and $Z = 0$ (right-hand panel). The plots refer to the point in each simulation at which 19 $M_\odot$ of material has been accreted (which occurs at a slightly different time in each simulation). The mass resolutions are 0.002 $M_\odot$ and 0.025 $M_\odot$ for the high and low resolution simulations, respectively. Note the similarity between the results of the low-resolution and high-resolution simulations. The onset of dust-cooling in the $Z = 10^{-5}\,Z_\odot$ cloud results in a stellar cluster which has a mass function similar to that for present day stars, in that the majority of the mass resides in the lower-mass objects. This contrasts with the $Z = 10^{-6}\,Z_\odot$ and primordial clouds, in which the bulk of the cluster mass is in high-mass stars. The figure is from Clark, Glover, & Klessen (2007).

The forming cluster represents a very extreme analogue of the clustered star formation that we know dominates in the present-day Universe (Lada & Lada 2003). A mere 420 years after the formation of the first object, the cluster has formed 177 stars (see Fig. 2). These occupy a region of only around 400 AU, or 2×10^{-3} pc, in size, roughly a hundredth of the size of the initial cloud. With $\sim 19\,M_\odot$ accreted at this stage, the stellar density is $2.25 \times 10^9\,M_\odot\,\mathrm{pc}^{-3}$. This is about five orders of magnitude greater than the stellar density in the Trapezium cluster in Orion (Hillenbrand & Hartmann 1998) and about a thousand times greater than that in the core of 30 Doradus in the Large Magellanic Cloud (Massey & Hunter 1998). This means that dynamical encounters will be extremely important during the formation of the first star cluster. The violent environment causes stars to be thrown out of the denser regions of the cluster, slowing down their accretion. The stellar mass spectrum thus depends on both the details of the initial fragmentation process (e.g. as discussed by Jappsen *et al.* 2005; Clark & Bonnell 2005) as well as dynamical effects in the growing cluster (Bonnell *et al.* 2001; Bonnell, Bate & Vine 2004). This is different to present-day star formation, where the situation is less clear-cut and the relative importance of these two processes may vary strongly from region to region (Krumholz, McKee, & Klein 2005; Bonnell & Bate 2006; Bonnell, Larson & Zinnecker 2007).

The mass functions of the protostars at the end of the $Z = 10^{-5}\,Z_\odot$ simulations (both high and low resolution cases) are shown in Fig. 4 (left-hand panel). When the simulation is terminated, collapsed cores hold $\sim 19\,M_\odot$ of gas in total. The mass function peaks somewhere below 0.1 $M_\odot$ and ranges from below $0.01\,M_\odot$ to about 5 $M_\odot$. This is not the final protostellar mass function. The continuing accretion of gas by the cluster will alter the mass function, as will mergers between the newly-formed protostars (which cannot be followed using our current sink particle implementation). Protostellar feedback in the form of winds, jets and H II regions may also play a role in determining the shape of the final stellar mass function. However, a key point to note is that the chaotic evolution of a bound system such as this cluster ensures that a wide spread of stellar masses will persist. Some stars will enjoy favourable accretion at the expense of others that will be thrown out of the system (as can be seen in Fig. 2), thus having their accretion effectively

terminated (see for example, the discussions in Bonnell & Bate 2006 and Bonnell, Larson & Zinnecker 2007). The survival of some of the low mass stars formed in the cluster is therefore inevitable.

In the $Z = 0$ and $Z = 10^{-6} \, Z_\odot$ calculations Clark, Glover, & Klessen (2007) find that fragmentation of the gas occurs as well, albeit at a much lower level than in the $Z = 10^{-5} \, Z_\odot$ run. The mass functions from these simulations are shown in Fig. 4 (middle and right-hand panels), and are again taken when $\sim 19 \, \mathrm{M}_\odot$ of gas has been accreted onto the sink particles, the same amount as is accreted by the end of the $Z = 10^{-5} \, Z_\odot$ calculations. Both distributions are considerably flatter than the present day IMF, in agreement with the suggestion that Population III stars are typically very massive. The fragmentation in the $Z = 10^{-6} \, Z_\odot$ simulation is slightly more efficient than in the primordial case, with 33 objects forming.

5. Conclusions

In this proceedings paper we have discussed several studies, where the thermodynamic behavior of the interstellar medium plays a crucial role in fragmentation and subsequent stellar birth. These examples range from star formation in the solar neighborhood at the present day to the formation of the very first stars in the early universe, and support the idea that the distribution of stellar masses depends, at least in part, on the thermodynamic state of the star-forming gas. Dips in the effective EOS, such that the relation between temperature T and density ρ changes from decreasing T with increasing ρ to increasing T with increasing ρ, i.e. the transition from a cooling ($\gamma < 1$) to a heating ($\gamma > 1$) regime, define a characteristic mass scale for fragmentation.

The thermodynamic state of interstellar gas is a result of the balance between heating and cooling processes, which in turn are determined by fundamental atomic and molecular physics and by chemical abundances. The derivation of a characteristic stellar mass can thus be based on quantities and constants that depend solely on the chemical abundances of the star forming gas. This is an attractive feature explaining the apparent universality of the IMF in the solar neighborhood as well as the transition from purely primordial high-mass star formation to the more normal low-mass mode observed today. Clearly more work needs to be done to investigate the validity of this hypothesis.

Acknowledgements

References

Abel, T., Bryan, G. L., & Norman, M. L. 2002, *Science*, 295, 93
Beers, T. C. & Christlieb, N. 2005, *ARA&A*, 43, 531
Bonnell, I. A., Clarke, C. J., Bate, M. R., & Pringle, J. E. 2001, *MNRAS*, 324, 573
Bonnell, I. A., Vine, S. G. & Bate, M. R. 2004, *MNRAS*, 349, 735
Bonnell, I. A. & Bate, M. R. 2006, *MNRAS*, 370, 488
Bonnell, I. A., Larson, R. B., & Zinnecker, H. 2007, Protostars and Planets V, B. Reipurth, D. Jewitt, and K. Keil (eds.), University of Arizona Press, Tucson, p. 149
Bromm, V., Ferrara, A., Coppi, P. S., & Larson, R. B. 2001, *MNRAS*, 328, 969
Bromm, V., Coppi, P. S., & Larson, R. B. 2002, *ApJ*, 564, 23
Bromm, V. & Loeb, A. 2003, *Nature*, 425, 812
Bromm, V. & Loeb, A. 2004, *New Astron.*, 9, 353
Chabrier, G. 2003, *PASP*, 115, 763

Christlieb, N., Bessell, M. S., Beers, T. C., Gustafsson, B., Korn, A., Barklem, P. S., Karlsson, T., Mizuno-Wiedner, M., & Rossi, S. 2002, *Nature*, 419, 904

Clark, P. C., & Bonnell, I. A. 2005, *MNRAS*, 361, 2

Clark, P. C., Glover, S. C. O., & Klessen, R. S. 2007, *ApJ*, in press; arXiv:0706.0613

Evans, N. J. 1999, *ARA&A*, 37, 311

Evans, N. J., Rawlings, J. M. C., Shirley, Y. L., & Mundy, L. G. 2001, *ApJ*, 557, 193

Frebel, A., Johnson, J. L., & Bromm, V. 2007, astro-ph/0701395

Glover, S. C. O. 2005, *Space Sci. Reviews*, 117, 445

Glover, S. C. O. & Mac Low, M.-M. 2007, *ApJ*, 659, 1317

Hayashi, C. 1966, *ARA&A*, 4, 171

Hayashi, C. & Nakano, T. 1965, *Prog. Theor. Phys.*, 34, 754

Heger, A. & Woosley, S. E. 2002, *ApJ*, 567, 532

Hillenbrand, L. A. & Hartmann, L. W. 1998, *ApJ*, 492, 540

Jappsen, A.-K., Klessen, R. S., Larson, R. B., Li, Y., & Mac Low, M.-M. 2005, *A&A*, 435, 611

Komiya, Y., Suda, T., Minaguchi, H., Shigeyama, T., Aoki, W., & Fujimoto, M. Y. 2007, *ApJ*, 658, 367

Koyama, H. & Inutsuka, S. 2000, *ApJ*, 532, 980

Kroupa, P. 1998, *MNRAS*, 298, 231

Kroupa, P. 2002, *Science*, 295, 82

Krumholz, M. R., McKee, C. F., & Klein, R. I. 2005, *Nature*, 438, 332

Krumholz, M. R. 2006, *ApJ*, 641, L45

Lada, C. J. & Lada, E. A. 2003, *ARA&A*, 41, 57

Larson, R. B. 1969, *MNRAS*, 145, 271

—. 1973b, *Fundamentals of Cosmic Physics*, 1, 1

—. 1985, *MNRAS*, 214, 379

—. 2005, *MNRAS*, 359, 211

Li, Y., Klessen, R. S., & Mac Low, M.-M. 2003, *ApJ*, 592, 975

Loeb, A. & Barkana, R. 2001, *ARA&A*, 39, 19

Low, C. & Lynden-Bell, D. 1976, *MNRAS*, 176, 367

Lucatello, S., Tsangarides, S., Beers, T. C., Carretta, E., Gratton, R. G., & Ryan, S. G. 2005, *ApJ*, 625, 825

Massey, P. & Hunter, D. A. 1998, *ApJ*, 493, 180

Masunaga, H. & Inutsuka, S. 2000, *ApJ*, 531, 350

Myers, P. C. 1978, *ApJ*, 225, 380

Omukai, K., Tsuribe, T., Schneider, R., & Ferrara, A. 2005, *ApJ*, 626, 627

O'Shea, B. W. & Norman, M. L. 2007, *ApJ*, 654, 66

Ryan, S. G., Aoki, W., Norris, J. E., & Beers, T. C. 2005, *ApJ*, 635, 349

Santoro, F. & Shull, J. M. 2006, *ApJ*, 643, 26

Scalo, J. 1998, in ASP Conf. Ser. 142: The Stellar Initial Mass Function (38th Herstmonceux Conference), ed. G. Gilmore & D. Howell (San Francisco: Astron. Soc. Pac.), 201

Schneider, R., Ferrara, A., Natarajan, P. & Omukai, K. 2002, *ApJ*, 571, 30

Schneider, R., Omukai, K., Inoue, A. K., & Ferrara, A. 2006, *MNRAS*, 369, 1437

Tafalla, M., Myers, P. C., Caselli, P., & Walmsley, C. M. 2004, *A&A*, 416, 191

Tan, J. C. & Blackman, E. G. 2004, *ApJ*, 603, 401

Tsuribe, T. & Omukai, K. 2006, *ApJ*, 642, L61

Widrow, L. M. 2002, *Rev. Mod. Phys.*, 74, 775

Yoshida, N., Omukai, K., Hernquist, L., & Abel, T. 2006, *ApJ*, 652, 6

Zucconi, A., Walmsley, C. M., & Galli, D. 2001, *A&A*, 376, 650